J. Phys. A 2, 157 (1969).
[9]A detailed account of the calculations described here will be given elsewhere.
[10]Similar arguments based on rotational invariance have been used by B. I. Halperin, P. C. Hohenberg, and E. D. Siggia, Phys. Rev. B 13, 1299 (1976), in an analysis of planar spin antiferromagnets.
[11]K. G. Wilson and J. Kogut, Phys. Rep. 12C, 77 (1974); M. W. Fisher, Rev. Mod. Phys. 42, 597 (1974); S. K. Ma, Rev. Mod. Phys. 45, 589 (1973).
[12]F. Wegner, Phys. Rev. B 5, 4529 (1972).
[13]Y. Pomeau and P. Résibois, Phys. Rep. 19C, 64 (1975).
[14]P. G. Wolynes, Phys. Rev. A 11, 1700 (1975).
[15]See, e. g., S. Coleman, in *Properties of the Fundamental Interactions, 1971*, edited by A. Zichichi (Editrice Compositori, Bologna, Italy, 1972), Part A, p. 358; H. D. Politzer, Phys. Rep. 14C, 131 (1974).

Anomalous Transport and Stabilization of Collisionless Drift-Wave Instabilities*

W. W. Lee and H. Okuda
Plasma Physics Laboratory, Princeton University, Princeton, New Jersey 08540
(Received 10 November 1975)

The nonlinear evolution of collisionless drift-wave instabilities and the associated plasma transport have been studied extensively using particle-code simulations. It is found that the quasilinear decay of the density profile gives rise to the nonlinear saturation. The results also indicate that a new mechanism of wave absorption is responsible for the observed anomalous energy transport, which, in general, is larger than the corresponding particle diffusion and is also less sensitive to shear.

Low-frequency gradient-driven microinstabilities in a magnetically confined plasma have attracted wide-spread interest in recent years in view of the fact that the resulting enhanced plasma transport is detrimental to confinement.[1,2] While much of the theoretical work has been directed at obtaining relevant stability criteria for these modes,[2] their nonlinear behavior and the associated plasma transport processes are far less understood.[1,3,4] It is generally believed that particle-code simulations should play a key role in helping us to gain insight into these areas and should provide guidelines for the analytic work.

With that in mind, we have conducted extensive numerical studies on the drift-wave instability driven by the finite-Larmor-radius effects in a low-β collisionless plasma (universal mode), using a newly developed particle-simulation code.[5] In this Letter, we will report on the comparisons of our results with the existing linear theories.[6-8] Such comparisons so far are unavailable from laboratory experiments.[9,10] We will also present results concerning the nonlinear behavior of the instability with regard to the mechanisms for the nonlinear saturation and the anomalous plasma transport, and the scaling laws in the presence of shear. It is our opinion that these results will have an important influence on the future development of the nonlinear theory for the gradient-driven microinstabilities.

A $2\frac{1}{2}$ dimensional (x, y, v_x, v_y, v_z) bounded-plasma model capable of handling a nonuniform system has been developed for our purpose.[5] The system is uniform and periodic in y, and is nonuniform in x where the plasma is bounded between two conducting walls. The main magnetic field $\vec{B}_0$ is perpendicular to the inhomogeneous x direction with $B_{0z} \gg B_{0y}$. Particles reaching the walls are reflected so as not to produce sheath currents and other undesirable effects.[5]

Let us first present a linear theory pertaining to our model. For the case of the universal mode, the governing equation for the perturbed potential $\varphi = \tilde{\varphi}(x)\exp(ik_y y - i\omega t)$ can be written as[4]

$$\sum_\alpha \frac{1}{T_\alpha}\left[1 + \frac{\omega + \omega_\alpha^*}{\sqrt{2}\,k_\parallel v_{t\alpha}} I_0(\hat{b}_\alpha) e^{-\hat{b}_\alpha} Z\left(\frac{\omega}{\sqrt{2}\,k_\parallel v_{t\alpha}}\right)\right]\tilde{\varphi} = 0, \qquad (1)$$
$$\hat{b}_\alpha = \rho_\alpha^2(k_y^2 - \partial^2/\partial x^2) = b_\alpha - \rho_\alpha^2\,\partial^2/\partial x^2,$$

where α denotes the species, $v_{t\alpha} = (T_\alpha/m_\alpha)^{1/2}$, $\rho_\alpha = v_{t\alpha}/\omega_{c\alpha}$, $\omega^* = k_y T_e \kappa/m_i\omega_{ci}$, $\omega_e^* = -\omega^*$, $\omega_i^* = \omega^* T_i/T_e$, $\kappa = -(dn/dx)/n$, $L_n \equiv 1/|\kappa|$ is the density scale length, $k_\parallel = k_y \cos\theta$, where θ is the angle between $\vec{k}$ and $\vec{B}_0$, I_l is the Bessel function, and Z is the plasma dispersion function.[11] Expanding Eq. (1) in the

limit of $k_x\rho_\alpha < 1$, we obtain the usual mode equation of the form

$$d^2\tilde{\varphi}/dx^2 + Q(x,\omega)\tilde{\varphi} = 0 . \tag{2}$$

We will now consider the solutions of Eq. (2) for several different cases. For a shear-free and constant-ω^* (or κ) case, Eq. (2) can be solved with the boundary conditions $\tilde{\varphi}(0) = \tilde{\varphi}(L_x) = 0$, and the resulting dispersion relation is similar to Eq. (1) with $-\partial^2/\partial x^2$ now replaced by $k_x^2 \equiv (m\pi/L_x)^2$ for $m = 1, 2, 3, \ldots$. The normal modes are given by

$$\tilde{\varphi} = \sin(m\pi x/L_x) . \tag{3}$$

For the case of a spatially dependent ω^* without shear, we expand Q in Eq. (2) around the maximum ω^* at x_1,[8] i.e., $\omega_\alpha^*(x) = \omega_{1\alpha}^* + \omega_{1\alpha}^{*\prime\prime}(x-x_1)^2/2$, and obtain

$$Q = A + B^2(x-x_1)^2 = \frac{\sum_\alpha [1 + (\omega + \omega_{1\alpha}^*)X_{0\alpha} + \omega_{1\alpha}^{*\prime\prime}X_{0\alpha}(x-x_1)^2/2]/T_\alpha}{\sum_\alpha \rho_\alpha^2(\omega + \omega_{1\alpha}^*)(X_{0\alpha} - X_{1\alpha})/T_\alpha} , \tag{4}$$

where $X_{l\alpha} = I_l(b_\alpha)\exp(-b_\alpha)Z(\omega/\sqrt{2}\,k_\parallel v_{t\alpha})/\sqrt{2}\,k_\parallel v_{t\alpha}$. The dispersion relation and the localized normal modes are, from Eqs. (2) and (4),

$$A = i\sigma(2l+1), \quad l = 0, 1, 2, \ldots, \tag{5}$$

and

$$\tilde{\varphi} = H_l((i\sigma)^{1/2}(x-x_1))\exp[-i\sigma(x-x_1)^2/2], \tag{6}$$

respectively, where H_l is the Hermite polynomial and $\sigma = \pm B$. The choice of sign for σ is such that $\mathrm{Im}\,\sigma < 0$ as required from the proper boundary conditions for outgoing waves at large x.[7,12]

To simulate a collisionless plasma,[13] the standard dipole-expansion technique with finite-size particles is used.[14] The guiding centers of the particles are loaded initially according to a prescribed density profile and with spatially uniform temperatures on a 64×32 ($L_x \times L_y$) spatial grid. Maxwellian velocity distributions are also used. The parameters of the simulations are $m_i/m_e = 25$, $T_e/T_i = 4$, $\lambda_{De}/\Delta = 2$, $\omega_{ce}/\omega_{pe} = 2$, the average number density $\langle n\rangle = 8/\Delta^2$, and a(rms of a Gaussian particle) $= 1.5\Delta$. The mesh size Δ is taken as the unit length. All the frequencies are measured in terms of ω_{pe}. These parameters give $k_x\rho_i = 0.12m$ and $k_y\rho_i = 0.49n$ where $m, n = 1, 2, 3, \ldots$. Exact dynamics for the particle pushing have been used with $\Delta t = 0.5$.

Two different density profiles have been used in the calculations; the exponential profile given by $\bar{n}_0(x, t=0) = \langle n\rangle \kappa L_x \exp(-\kappa x)/[1 - \exp(-\kappa L_x)]$ with $\kappa = 0.07$ and the hyperbolic tangent profile given by $\bar{n}_0(x, t=0) = \langle n\rangle\{1 - \kappa_0 l_0 \tanh[(x-x_0)/l_0]\}$ with $\kappa_0 = 0.1$, $l_0 = 24/\pi$, and $x_0 = 32$, as shown in Fig. 1(a). For the exponential profile in which ω^* is constant, the most unstable mode, from Eq. (1), is found to be $(m, n) = (1, 1)$ with $\omega = 0.0064$ and $\gamma = 0.0048$ for $\theta = 88.5°$. For the case of the hyperbolic tangent profile, ω^* has a peak at $x_1 = 36$ where $\kappa_{\max} = 0.12$ and $\kappa_{\max}'' = -0.0033$. Equation (5) gives $\omega = 0.0055$ and $\gamma = 0.0048$ for the most unstable mode $(l, m) = (0, 1)$ for $\theta = 88.5°$. Since the two growth rates are the same, we define $\langle L_n\rangle = 1/0.07$ as the average density scale length to describe both systems.

The simulation results of the growth rates for the two density profiles, measured in terms of the average density modulation versus time, are shown in Fig. 1(b) where $\langle \bar{n}_1(x,t)\rangle = \int \bar{n}_1(x,t)\,dx/L_x$ is the spatial average of the most unstable $n = 1$ mode. The agreement with theory is excellent. The instability grows above the thermal noise at $t = 400$ and exponentiates at the expected growth rate. The saturation density modulation is about 10%. The corresponding frequencies are found to be $\omega = 0.004$ for both cases at $t = 1200$ and are smaller than the theoretical estimates. This is due to the quasilinear diffusion to be discussed later.

The spatial structures of $n = 1$ mode are shown in Fig. 1(c). For the exponential profile case, several normal modes in x have initially been excited which are eventually dominated by the $m = 1$ mode at $t = 880$. The deviation of the mode structure from Eq. (3) is again due to the quasilinear diffusion. For the hyperbolic tangent profile case, $l = 0$ is the only unstable mode and its structure at the linear stage of the instability, $t = 560$, agrees very well with that given by Eq. (6).

As the instability develops, the density profile undergoes a quasilinear change in time due to the $\vec{E}\times\vec{B}$ drift as shown in Fig. 1(a). Initially, the diffusion takes place at around the maximum wave amplitude, then gradually evolves into a plateau, and finally settles into a new stable configuration. The density profiles then oscillate around the new equilibrium with approximately

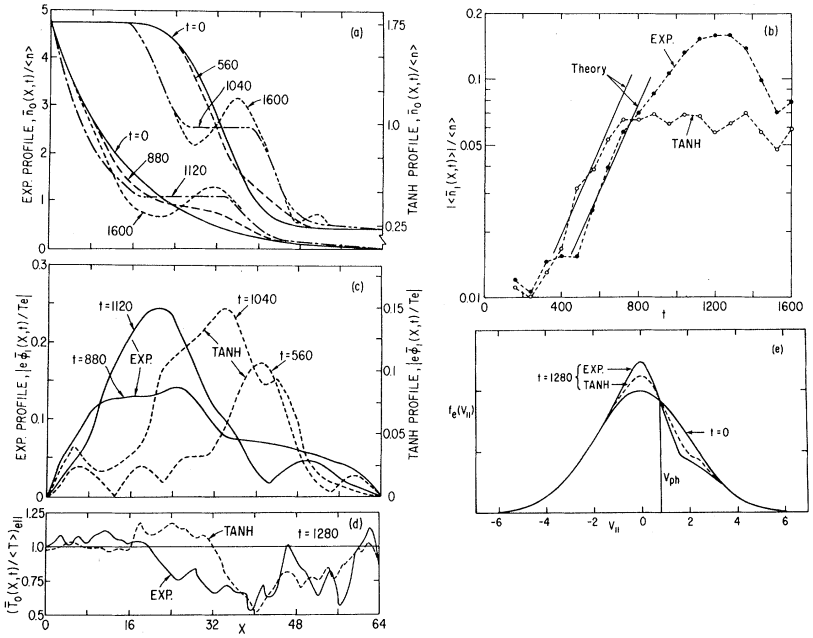

FIG. 1. (a) Time evolution of the density profiles. (b) Growth of the density modulation for $n=1$ mode. (c) Mode structures for $n=1$ mode. (d) Parallel electron heat transfer patterns. (e) Average velocity distributions.

twice the drift frequency because of the existence of the large-amplitude waves in the system by this time. The profiles shown for $t=1600$ roughly correspond to the equilibrium states. The solutions from Eq. (5) have confirmed this observation; i.e., these final configurations are indeed linearly stable. In general, the diffusion of the electrons is found to be slower than that of the ions. The amplitude of the modes has reached a maximum at the time of the plateau formation with $e\bar{\varphi}_1/T_e=25$ and 15%, respectively, for the two cases. Note the initial noise level here is about 1.5%.

Let us now examine the energy transport processes associated with the instability which were first pointed out by Coppi.[15] The simulation results have shown that in the linear stage there is energy transfer from the parallel electron temperature to the waves through inverse Landau damping in the unstable regions. However, as the waves grow in amplitude causing the quasilinear diffusion, a significant amount of electron heating has been observed elsewhere. After the plasma reaches the stable configuration, the heating also stops. The electron heat transfer patterns normalized by the initial temperature $\langle T\rangle_{e\parallel}$ are shown in Fig. 1(d). The energy loss from the unstable regions is about 10% of the total parallel electron thermal energy for the exponential case and 7% for the other. More than half of that amount, however, is transported by the waves back to the electrons in other regions causing large heat transfer. This is due to the quasilinear change in density which alters the local dispersions; however, the linear wave absorption is also responsible for the heating in the hyperbolic tangent case.[15] Most of the remaining amount goes to the ambipolar drift, and relatively little is kept by the waves. No ion heating has been detected, except for the ion drift parallel to $\vec{B}_0$. In Fig. 1(e), the average electron velocity distribution functions corresponding to those in Fig. 1(d) are shown along with the measured phase velocity. The resonance regions are evidently broadened by the instability. This is also the case for the local distributions.

The nonlinear behavior of the instability reported here does not seem to agree with the various existing theories.[1,3,4] Instead, the quasilinear diffusion in space is the dominant saturation mechanism. The theoretical analysis has been initiated with encouraging results and will be reported later.[16]

Let us now look at the shear stabilization of drift waves using the hyperbolic tangent density profile. The sheared magnetic field is introduced by adding $\vec{B}_s(x)=\hat{y}B_0(x-x_1)/L_s$ to $\vec{B}_0$. We choose $x_1=36$ so that $B_s=0$ at the maximum κ. As the shear length decreases, we have observed a reduction in the associated plasma transport with

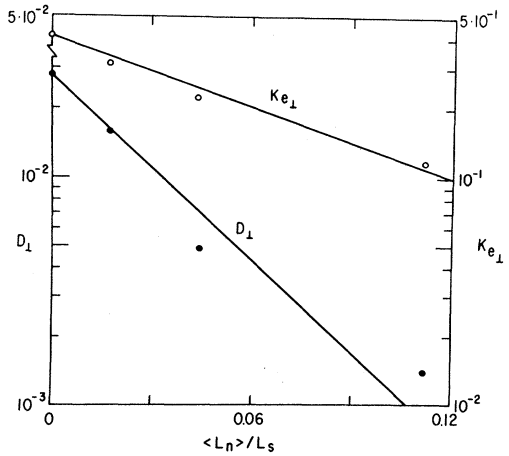

FIG. 2. Diffusion and conductivity coefficients versus shear.

the overall patterns similar to those of the shearless case. Again, no ion heating has been detected. The results also indicate that the saturation for the partially stabilized drift waves is due to the quasilinear density decay.

To estimate the particle diffusion and heat conductivity coefficients, the diffusion equation, $\partial(\bar{n}_0, \bar{T}_{e\parallel})/\partial t = (D_\perp, K_{e\perp})\partial^2(\bar{n}_0, \bar{T}_{e\parallel})/\partial x^2$, is used. The average coefficients versus shear for the hyperbolic tangent profile are shown in Fig. 2. For the shear-free case, the measured $D_\perp$ is about 25% of the values given by the Bohm diffusion, $D_\perp \sim cT_e/16eB_0$, and the turbulent diffusion, $D_\perp \sim \gamma/k_\perp^2$, by Kadomtsev,[1] while $K_{e\perp}$ is about four times bigger. These are also true for the shear-free exponential case. The Pearlstein and Berk criterion for the total stabilization by shear[7] is $\langle L_n\rangle/L_s \geq 0.24$ for our case. The results shown in Fig. 2 approach this limit asymptotically if extrapolation is used. However, our results differ from the estimate given by Ref. 8. Figure 2 also shows that the heat conductivity for the electrons is much less sensitive to shear.

The detailed comparison of the simulation results with the theory for the shear stabilization will be reported in a separate paper.[12]

The authors wish to acknowledge useful discussions with Dr. C. Oberman, Dr. Y. Y. Kuo, and Dr. W. M. Tang.

---

*Work supported by the U. S. Energy Research and Development Administration Contract No. E(11-1)-3073.

[1]B. B. Kadomtsev, *Plasma Turbulence* (Academic, New York, 1965), Sects. IV. 3 and IV. 4.

[2]A. B. Mikhailovskii, *Theory of Plasma Instabilities*, translated by J. B. Barboar (Consultants Bureau, New York, 1974), Vol. II.

[3]R. Z. Sagdeev and A. A. Galeev, in *Nonlinear Plasma Theory*, edited by T. M. O'Neil and D. L. Book (Benjamin, New York, 1969), Sects. II.6 and III.3.

[4]T. H. Dupree, Phys. Fluids 9, 1773 (1966), and 10, 1049 (1967), and 11, 2680 (1968).

[5]W. W. Lee and H. Okuda, Princeton Plasma Physics Laboratory Report No. MATT 1231 (to be published).

[6]N. A. Krall and M. N. Rosenbluth, Phys. Fluids 8, 1488 (1968), and references therein.

[7]L. D. Pearlstein and H. L. Berk, Phys. Rev. Lett. 23, 220 (1969).

[8]N. R. Sauthoff, M. Okabayashi, and J. A. Schmidt, Phys. Fluids 18, 915 (1975).

[9]P. A. Politzer, Phys. Fluids 14, 2410 (1971).

[10]P. E. Stott, P. F. Little, and J. Burt, Phys. Rev. Lett. 25, 996 (1970).

[11]B. D. Fried and S. D. Conte, *The Plasma Dispersion Function* (Academic, New York, 1961).

[12]Investigation by W. M. Tang and the authors.

[13]Y. Matsuda and H. Okuda, Phys. Fluids 18, 1740 (1975).

[14]H. Okuda and J. M. Dawson, Phys. Fluids 16, 408 (1973).

[15]B. Coppi, Phys. Rev. Lett. 25, 851 (1970).

[16]Y. Y. Kuo, W. W. Lee, and H. Okuda, to be published.